QUANTIFYING THE INFLUENCE OF NEAR-SURFACE WATER-ENERGY BUDGETS ON SOIL THERMAL PROPERTIES USING A NETWORK OF COUPLED METEOROLOGICAL AND VADOSE-ZONE INSTRUMENT ARRAYS IN INDIANA, USA

CENTER FOR GEOSPATIAL DATA ANALYSIS
INDIANA UNIVERSITY

Shawn Naylor (snaylor@indiana.edu), Center for Geospatial Data Analysis, Indiana Geological Survey, Indiana University, Bloomington, Indiana.
Andrew R. Gustin (angustin@indiana.edu), Center for Geospatial Data Analysis, Indiana Geological Survey, Indiana University, Bloomington, Indiana.
Kevin M. Ellett (kmellett@indiana.edu), Indiana Geological Survey, Indiana University, Bloomington, Indiana.

Abstract ID: H31G-1195

Weather stations that collect reliable, sustained meteorological data sets are becoming more widely distributed because of advances in both instrumentation and data server technology. However, sites collecting soil moisture and soil temperature data remain sparse with even fewer locations where complete meteorological data are collected in conjunction with soil data. Thanks to the advent of sensors that collect continuous in-situ thermal properties data for soils, we have gone a step further and incorporated thermal properties measurements as part of hydrologic instrument arrays in central and northern Indiana. The coupled approach provides insights into the variability of soil thermal conductivity and diffusivity attributable to geologic and climatological controls for various hydrogeologic settings. These data are collected to facilitate the optimization of ground-source heat pumps (GSHPs) in the glaciated Midwest by establishing publicly available data that can be used to parameterize system design models.

A network of six monitoring sites was developed in Indiana. Sensors that determine thermal conductivity and diffusivity using radial differential temperature measurements around a heating wire were installed at 1.2 meters below ground surface— a typical depth for horizontal GSHP systems. Each site also includes standard meteorological sensors for calculating reference evapotranspiration following the methods by the Food and Agriculture Organization (FAO) of the United Nations. Vadose zone instrumentation includes time domain reflectometry soil-moisture and temperature sensors installed at 0.3-meter depth intervals down to a 1.8-meter depth, in addition to matric potential sensors at 0.15, 0.3, 0.6, and 1.2 meters. Cores collected at 0.3-meter intervals were analyzed in a laboratory for grain size distribution, bulk density, thermal conductivity, and thermal diffusivity.

Our work includes developing methods for calibrating thermal properties sensors based on known standards and comparing measurements from transient line heat source devices. Transform equations have been developed to correct in-situ measurements of thermal conductivity and comparing these results with soil moisture data indicates that thermal conductivity can increase by as much as 25 percent during wetting front propagation. Thermal dryout curves have also been modeled based on laboratory conductivity data collected from core samples to verify field measurements, and alternatively, temperature profile data are used to calibrate near-surface temperature gradient models. We compare data collected across various spatial scales to assess the potential for upscaling near-surface thermal regimes based on available soils data. A long-term goal of the monitoring effort is to establish continuous data sets that determine the effect of climate variability on soil thermal properties such that expected ranges in thermal conductivity can be used to determine optimal ground-coupling loop lengths for GSHP systems.

In-situ thermal properties measurement

The Hukseflux TP01 utilizes dual thermopiles providing radial temperature measurement around a heating wire to determine thermal conductivity (λ) and diffusivity (α).

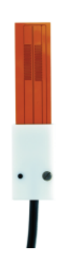

$V \sim 1/\lambda$ — *A.* Following an initial transition period, temp. rise close to the heating element is a function of the thermal conductivity of the soil medium (λ) and is no longer dependent on heat capacity.

$t \sim \alpha$ — *B.* The time response of the probe during the transition period ($t\lambda_x$ in fig. below) is proportional to the diffusivity of the surrounding medium.

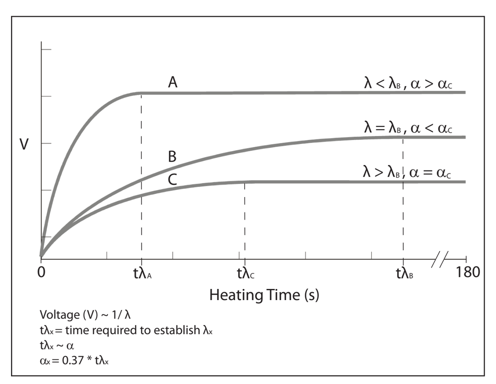

Figure 1. TP01 thermal conductivity and diffusivity measurement approach. (modified from Hukseflux, 2012)

$$\underbrace{U - U_0 = (E_\lambda Q/\lambda)}_{A.}\ \underbrace{F(\alpha t)}_{B.}$$

U = thermopile voltage reading
U_0 = initial voltage
Q = power applied
E_λ = factory calibration constant
λ = thermal diffusivity
t = time
F = function equal to 1 for large αt

Calibrations

-Since previous researchers (Liebethal and Foken, 2006) have observed underestimates of λ and unreliable results for α using the TP01 in field settings, we undertook a rigorous calibration exercise using both the TP01 and Decagon's KD2-Pro sensor that employs the transient line heat source method for determining λ and α.

-Standards with previously published l values were measured with all instruments (all 6 TP01 sensors were used).

-Glycerin (0.285 W/mK)
-Ottawa sand (dry) (0.332 W/mK)
-Agar gel (5%) (0.554 W/mK)
-Agar gel (0.5%) (0.598 W/mK)
-Ottawa sand (saturated) (3.310 W/mk)

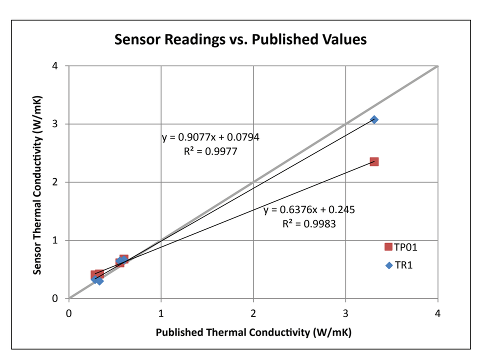

Figure 2. Hukseflux TP01 and Decagon KD2-Pro TR-1 sensor calibration results

-Using the standards and lab soil samples, a transform was developed between instruments to correct for the underestimated TP01 readings.

-Our laboratory calibration results were consistent with Liebethal and Foken (2006) who found that the TP01 underestimated λ by 31%.

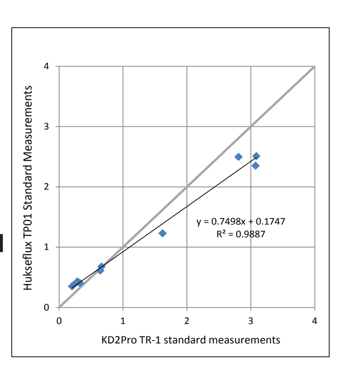

Figure 3. Transform equation developed to correct for underestimated TP01 readings

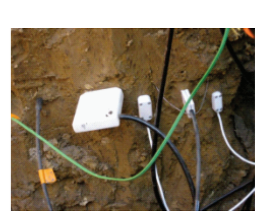

Table 1. In-situ comparison of TP01 and transient line heat source sensor readings.

	Thermal conductivity			Diffusivity	
	Decagon KD2-Pro TR-1	Hukseflux TP-01 corrected	error	Decagon KD2-Pro SH-1	Hukseflux TP-01 corrected
Date	(W/mK)	(W/mK)	%	(mm^2/s)	(mm^2/s)
12/25/11	1.64	1.77	8.5%	0.718	0.375
7/21/12	1.58	1.71	8.0%	0.659	0.375
8/27/12	1.59	1.69	5.9%	0.625	0.375
9/4/12	1.55	1.69	8.7%	-	-
9/13/12	1.55	1.69	9.0%	0.652	0.375
9/19/12	1.56	1.69	8.2%	0.645	0.375
9/27/12	1.57	1.69	8.1%	0.638	0.375
9/28/12	1.58	1.69	7.4%	0.643	0.375
10/1/12	1.59	1.70	7.0%	0.64	0.375

–We installed Decagon single- and dual-needle sensors adjacent to the TP01 sensor at site# 3 to compare in-situ readings using both methods.
-Transform-corrected TP01 λ readings were within 9% of single needle measurements.
-Precision of TP01 α readings were limited by the time step used in the datalogger program.
-Previous researchers (Tikhonravova, 2007) measured a of clay loam soils between 0.15 and 0.30 mm^2/s indicating that the TP01 provides better in-situ a results than the Decagon dual-needle SH-1 sensor.

Monitoring sites

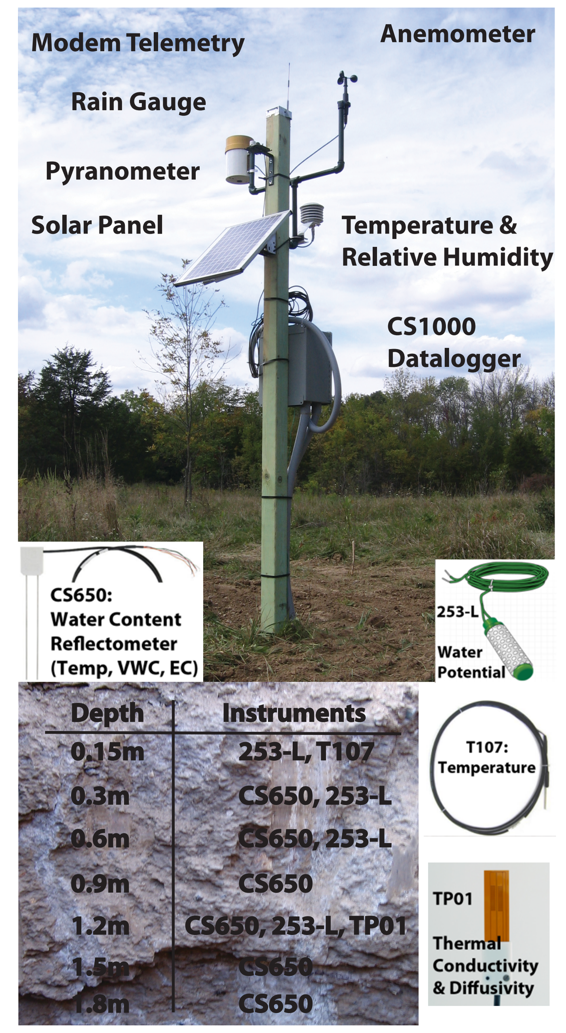

Figure 4. Meteorological and vadose-zone instruments installed at each site.

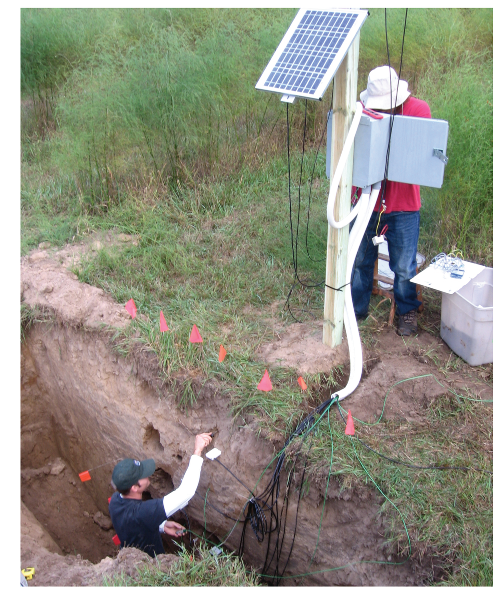

Figure 5. Photograph showing installation of subsurface instruments into trench face.

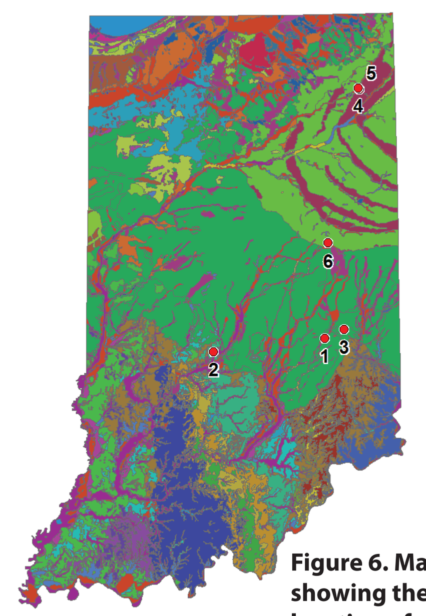

Figure 6. Map showing the location of six monitoring sites and the diversity of surficial geology in Indiana.

Table 1. Geologic settings and sedimentologic details for each monitoring site. Deep horizon soil texture and bulk density from the Soil Survey Geographic Database (SSURGO) are also shown for each location.

Site #	Site name	Geologic setting	Deep horizon texture	Deep horizon bulk density (g/cm^3)	SSURGO deep horizon texture	SSURGO deep horizon bulk density (g/cm3)
1	Flatrock	low-level outwash terrace	sandy clay loam	TBD	stratified coarse sand to gravelly sand	2.06
2	Bradford	alluvial terrace	silt loam	1.39	stratified sandy loam to silt loam	1.62
3	Shelbyville	moraine crest	silty clay loam	1.71	loam	1.90
4	Eel River	high-level outwash terrace	sandy loam	1.69	stratified sand to silt loam	1.68
5	Wabash	moraine crest	clay loam	1.91	clay loam	2.06
6	Ball State	ground moraine	TBD	TBD	clay loam	2.07

Conductivity and diffusivity data

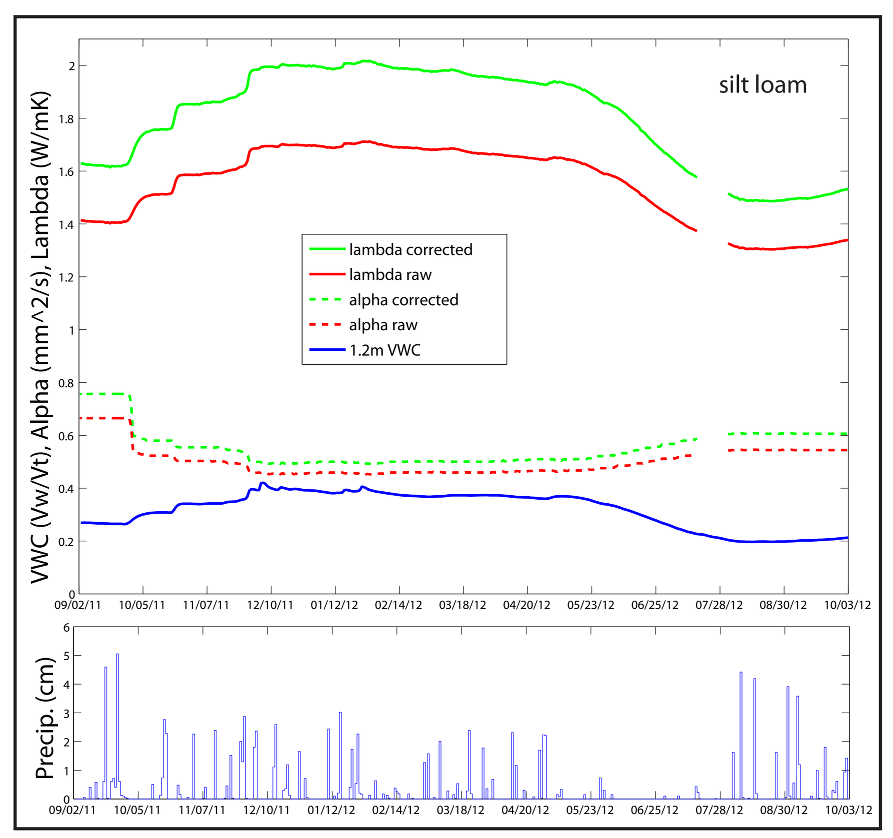

Figure 7. Bradford (site #2) thermal conductivity and diffusivity plotted with volumetric water content and precipitation.

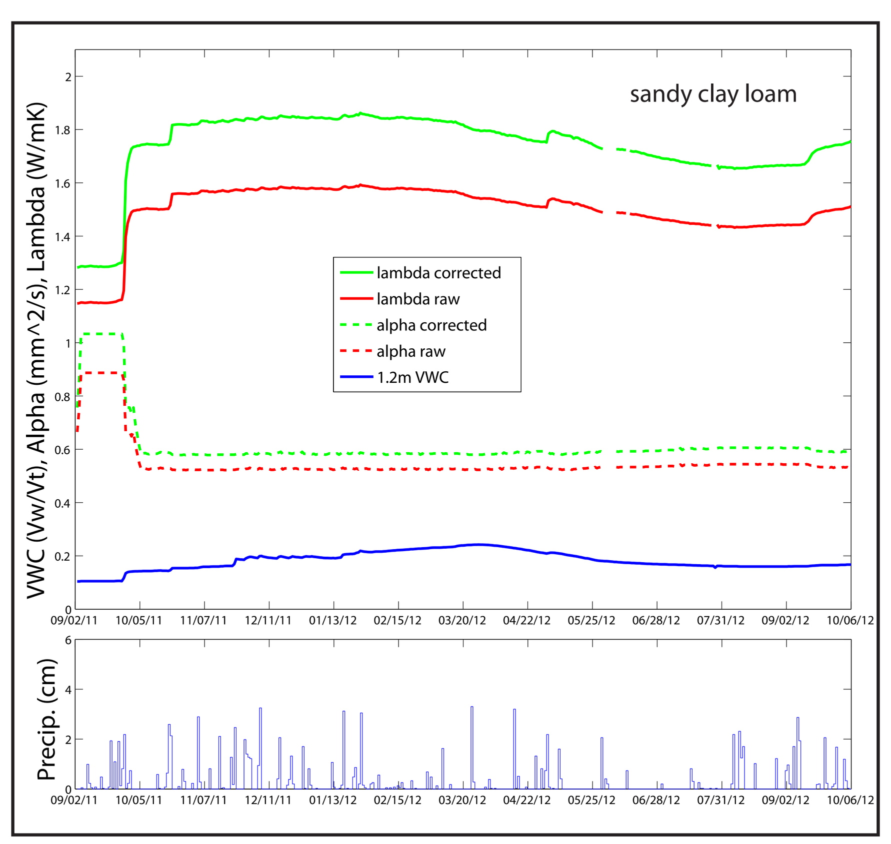

Figure 8. Flatrock (site #1) thermal conductivity and diffusivity plotted with volumetric water content and precipitation.

-Following a drought during mid-summer 2011, data for both the Eel River and Bradford sites showed a 25% increases in λ when late-summer rain events increased soil moisture at depth.

-1.2m θ lowered slightly at both the Eel River and Bradford sites following a second consecutive drought in the 2012 summer resulting in lower thermal conductivities than were measured in the previous summer.

-There is an inverse relationship when comparing α with λ and θ for all sites -- this is consistent with previous research (Tikhonravova, 2007; Yang and Koike, 2005) and we attribute it to the high specific heat capacity of pore water.

-The initial 50% increase in λ at the Flatrock site appears to be the result of installation conditions. In particular, we presume that contact resistance existed until the first wetting front propogated through the soil profile following rains in mid-late September, 2011.

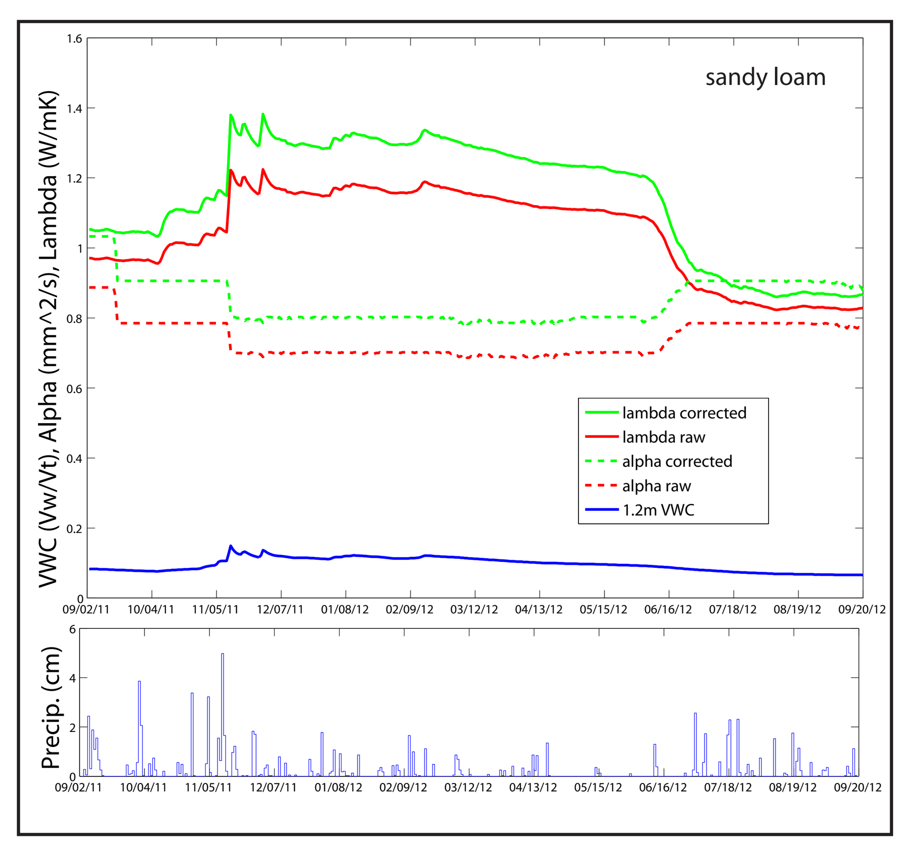

Figure 9. Eel River (site #4) thermal conductivity and diffusivity plotted with volumetric water content and precipitation.

Temperature profiles

Soil temperature measurements
- Continuous hourly data are collected at 15.25 cm, 30.5 cm, and at 30.5 cm increments down to 183 cm.

- Measured using Campbell T107 temperature probes at 15.25 cm and Campbell CS650 soil moisture probes at lower depths

Modeled temperature profiles
-Harmonic model from Hillel (1983) used to predict temperature profiles

$$T(z,t) = \bar{T} + A_0[sin(\omega t - z/d)]/e^{z/d}$$

$\bar{T}$ = avg. annual soil surface temp. (based on measured 15cm soil temp. at each site
A_0 = amplitude of surface temp. fluctuation
ω = radial frequency ($2\pi/365$)
z = depth
d = damping depth ($2\alpha/\omega$)

-Model parameters are based on empirical data as opposed to calibration procedures (T and A_0 are based on 15cm temp. and α is taken from trench face measurements)

-Modeled temp. profiles are shown for two monitoring site pairs with spacing within 15 km of one another to examine the potential for upscaling the sinusoidal estimates of near-surface temps. across geologic settings.

-The black line on 183cm plots (figs. 10 & 11) indicates typical temp. estimated during GSHP design.

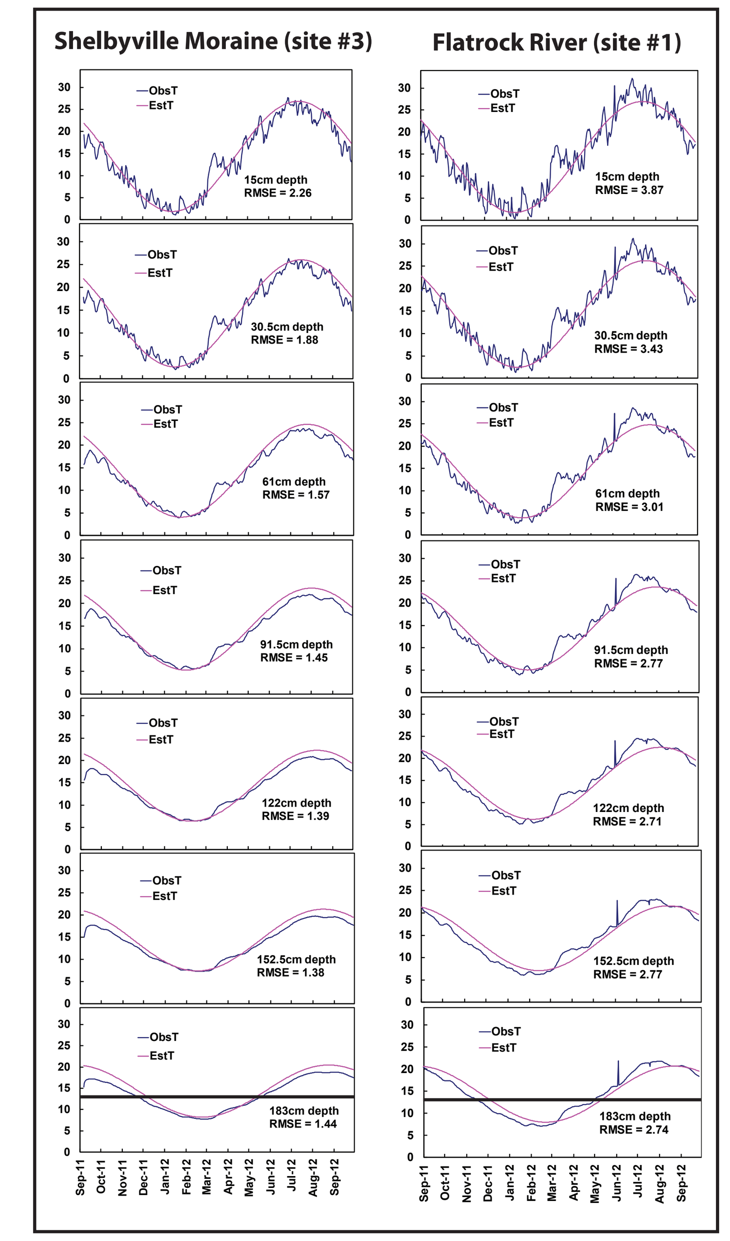

Figure 10. Observed and modeld temperature profiles for two sites in eastern Indiana (all temps. are in degrees Celsius).

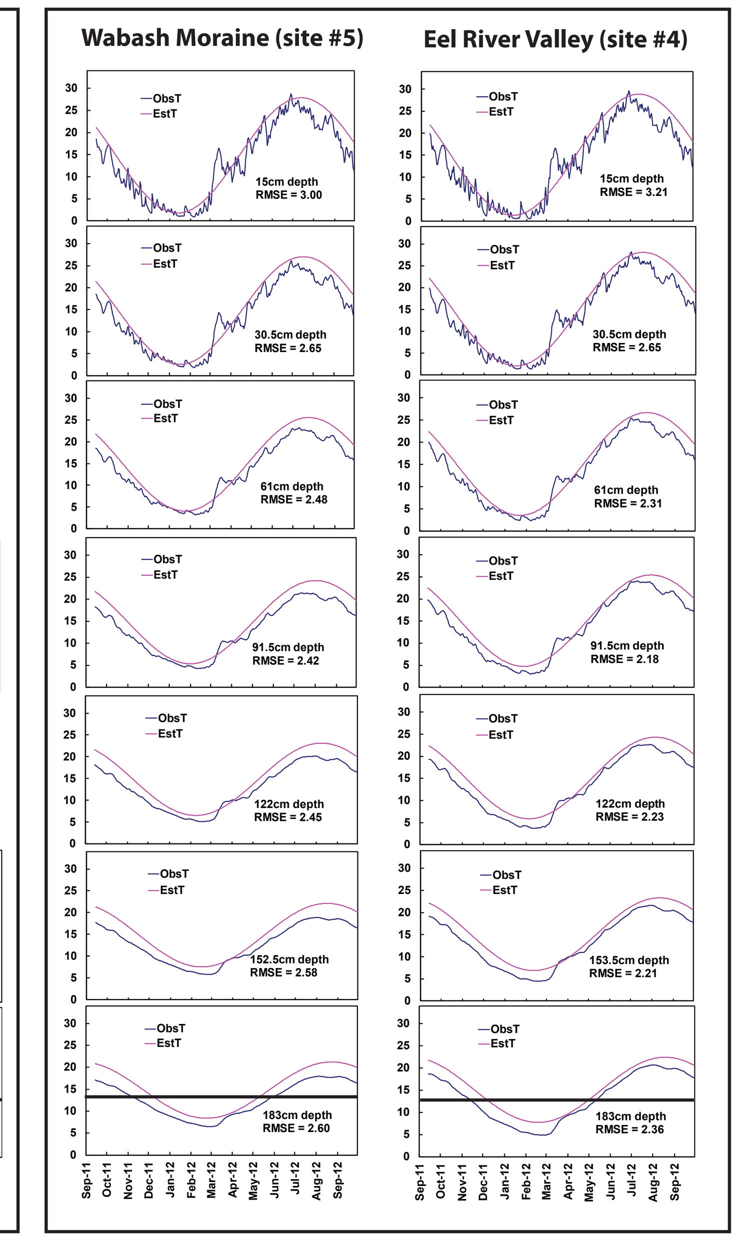

Figure 11. Observed and modeld temperature profiles for two sites in northern Indiana (all temps. are in degrees Celsius).

Thermal dryout curves

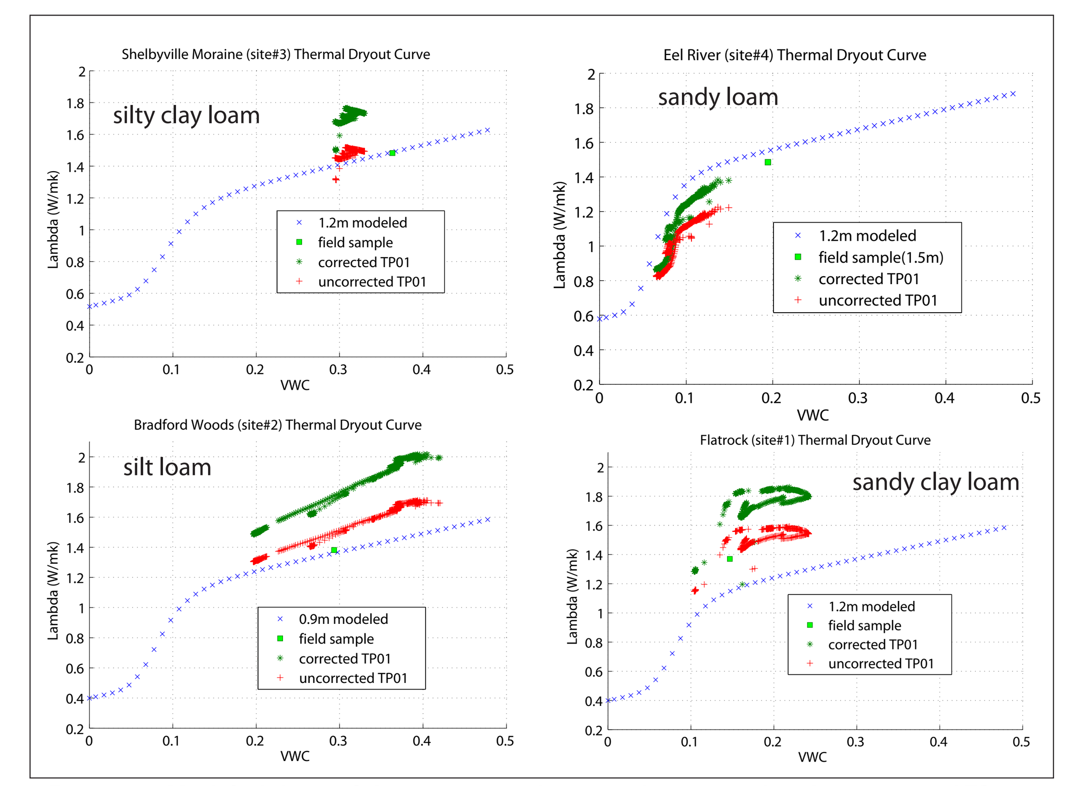

Figure 12. Modeled thermal dryout curves shown with corrected and uncorrected TP01 data along with data for a sample collected adjacent to TP01 sensor during installation.

Estimating the relationship between θ and λ for comparison with field measurements
-In lieu of painstakingly varying θ and repeating λ measurements, a method using equations from Campbell (1985) and Campbell et al. (1994) is used to estimate the relationship.
-$\lambda$is determined for both saturated and oven-dry soil samples in order to fix two points on the thermal dryout curve and the following equation is used to perform an interpolation between these points.

$$\lambda = \lambda_{wet} g + \lambda_{dry}(1 - g) + 2.8\phi(\theta - \theta_{wet} g)$$

λ = thermal conductivity ($W\ m^{-1}K^{-1}$)
λ_{wet} = thermal conductivity of wet soil
λ_{dry} = thermal conductivity of oven-dry soil
ϕ = total porosity
θ = water content
θ_{wet} = saturated water content

$$g = \frac{1}{1 + \left(\frac{\theta}{\theta_0}\right)^{-5}}$$

θ_0 = cutoff θ for soil liquid return flow (est. from clay content)

-Modeled curves for site#'s 2 and 3 indicate that uncorrected TP01 data are accurate. However, the site #4 curve shows that corrected data more closely match the modeled results.
-The site #1 curve significantly underestimates λ at all θ when compared to both TP01 data and the field sample. This may be the result of an undersaturated core λ measurement used to fix the wet end of the curve.

Discussion

Determining accuracy of TP01 sensors placed in-situ
-Laboratory λ standards measurements indicate that TP01 sensors underestimate λ by approximately 30%, consistent with previous findings by Lieberthal and Foken (2006), BUT...
-Field data indicate that underestimates only exist when contact resistance occurs with more granular sediments (Eel River, site# 4).
-Sensor transform equations are only necessary where low clay contents exist and; otherwise, sensors give reliable data.

Seasonal fluctuations in θ and the effect on λ and α
-A 100% increase in θ can result in a 30% decrease in λ and preliminary data indicate that such variation can occur annually for geologic settings with more granular sediment textures.
-Consistent with Yang and Koike (2005), a roughly inverse relationship exists between λ and α at certain moisture contents.

Potential for models to accurately predict temperature profiles and the relationship between θ and λ
-The traditional harmonic ground-temperature profile model can provide reasonably accurate profiles provided ground-surface temp. or very shallow subsurface (<15mm) temp. is measured.
-Modeled thermal dryout curves based on Campbell's (1985) method provide a relationship between θ and λ that is typically consistent with our measured data.

Conclusions / future work

-Summer λ values can be drastically different when compared to winter λ values indicating that GSHP designs should consider dual thermal regimes for certain geologic settings.
-Contrary to previous research, the Hukseflux TP01 sensor provides accuracy that is within 10% of line-source measurement methods provided contact resistance is not an issue.
-The dataset will allow us to develop a sensitivity ranking system that will indicate the relative dependence of λ on multiple variables: texture, bulk density, θ, and temperature.
-We plan to calibrate harmonic analytical solutions to the 1-dimensional heat flow equation such that widely available input data such as air temperature can be used to accurately estimate near-surface temperature profiles throughout Indiana.
-λ / θ plots indicate a dynamic relationship and we hope to discover whether this is due to temperature effects (Campbell et al., 1994) or soil tension hysteresis.

References

Campbell, G.S. (1985) Soil Physics with BASIC: Transport Models for Soil - Plant Systems. Elsevier, New York, 150 pp

Campbell, G.S., Jungbauer, J.D., Bidlake, W.R., and Hungerford, R.D. (1994) Predicting the effect of temperature on soil thermal conductivity. *Soil Science* **158**:5, 307-313

Hillel, D. (1983) Introduction to Soil Physics. Academic Press, New York, 364 pp

Hukseflux Thermal Sensors (2012) TP01 Thermal Properties Sensor product brochure. Downloaded from <http://www.hukseflux.com/product/tp01> on November 20, 2012.

Liebethal, C., and Foken, T. (2006) On the use of two repeatedly heated sensors in the determination of physical soil properties. *Meteorologische Zeitschrift* **15**:3, 293-299

Tikhonravova, P.I. (2007) Effect of the water content on the thermal diffusivity of clay loams with different degrees of salination in the Transvoga region. *Eurasian Soil Science* **40**:1, 47-50

Yang, K., and Koike, T. (2005) Comments on "Estimating soil water contents from soil temperature measurements by using an adaptive Kalman filter". *Journal of Applied Meterology* **44**:4, 546-550

Project sponsors and collaborators

This research was funded by a grant from the Geothermal Technologies Program of the U.S. Dept. of Energy to the Association of American State Geologists (prime award: DE-EE0002850, subaward:IN-0002850).